Structure and Properties of Some Metallic Biomaterials from System Ti-Nb-Fe Used in Implantology

CRISTIAN PREDESCU, SORIN CIUCA, ANDRA PREDESCU*, ALEXANDRA BANU, CRISTIAN PANTILIMON, ECATERINA MATEI, MIRELA SOHACIU, ANDREI BERBECARU, GEORGE COMAN
University Politehnica of Bucharest, 313 Splaiul Independentei, 060042, Bucharest, Romania

In this study special biomaterials from Ti-Nb-Fe system are obtained under two conditions of cooling from the liquid state. As a result of structural investigations, the constitution is biphasic $\alpha + \beta$ with a proportion of β phase increasing with cooling rate. Also, the corrosion tests demonstrate that obtained alloy by fast cooling rate had a better corrosion resistance.

Keywords: biomaterial; electron microscopy; corrosion; x-ray diffraction

Titanium and its alloys are well known like metallic materials having the higher biocompatibility, referential being Ti6Al4V alloy with phase $\alpha+\beta$ structure field [1-3]. The latest research reports that the Al and V ions can lead to various health problems [4-6]. Development of β alloys in the absence of toxic elements has carried out to fabrication of a new based Ti alloys which the elastic modulus closer to human bone (10-40 GPa) [7]. In order to maintain a high corrosion resistance and to determine a compatible elastic modulus some β stabilizer elements without toxic effect such as Nb and Fe were added [8]. The actual studies reveal that a concentration of less than 15 wt% Nb leads to the formation of a hexagonal α' Ti martensitic phase, while a concentration of 17.5-25 wt% Nb determines orthorhombic α" martensitic phase formation. Both of these are inadequate for medical applications. Only a Nb content over 30 wt% can lead to an almost complete equi-axed β phase [9], but at the risk of a higher cost. The influence of Fe content, on the Ti-Nb system has been studied regarding the structure and the corrosion resistance [10-12].

In this work, an economic metallic biomaterial from Ti-Nb-Fe system was obtained using a special casting process, which is able to achieve a high homogeneity and purity and to control the casting structure in order to obtain a predominant β phase. Concretely, our research was conducted to correlate the obtained structure with corrosion resistance in media simulating human body conditions and to establish the optimal casting parameters for the structure providing the better biocompatibility.

Experimental part

The Ti-Nb-Fe alloy was designed from 99.9% pure raw Ti, Fe and Nb metals using a cold crucible levitation melting furnace (Five Celles, ALU 600), under argon atmosphere. The parameters used for the process are as follows: nominal power (Pn) of 25 kW, vacuum of $5x10^{-5}$ bar and an argon atmosphere maintained at 1.1 bar. After the complete melting of the raw metals, two different samples were obtained: one of the sample containing the molten metal was solidified by controlled cooling inside a copper ingot (fast cooling) and the other was slow cooled under argon atmosphere. The casting temperature was 1975°C for a power of 24 kW; the raw materials were processed for 12 min with the following cooling rates: 40°C/min for slow cooling (*sample A1*) and 160°C/min for fast cooling (*sample A2*). The size of the alloy ingots was 17 mm in diameter and 50 mm length. The ingots were sectioned using cutting equipment for metallographic samples (Struers, Discotom 10) in order to obtain specimens for various purposes. Then, the samples were prepared for metallographic analysis. The first step in our investigation was to determine the chemical composition. The analysis was performed with an optical emission spectrometer-EOS (Leco, GDS 500 A), with a dispersive focal length of 0.225 m.

The phase constitution was identified by X-Ray diffraction - XRD using an X-ray diffractometer (Panalytical, X'Pert PRO MPD) with high-intensity Cu–Kα radiation (λ = 1.54065 A) and 2è range from 20 to 80° in order to obtain XRD patterns. For the purpose to assess the morphology and structure, SEM measurements were performed using a scanning electron microscope (FEI, Quanta 450 FEG), with a 1 nm resolution under high vacuum mode at 30 kV. The corrosion tests were conducted in order to establish the chemical behavior of the purposed metallic biomaterial. The electrochemical measurements were performed using a Gamry Reference 600 potentiostat/ galvanostat in a conventional three electrodes electrochemical system with: Saturated calomel electrode (SCE) as a reference electrode, Pt electrode as an auxiliary electrode and a 2 cm^2 working electrode. The ratio between work electrode surface and auxiliary electrode surface was 0.25. As corrosion solution was used a solution composed from 0.1M lactic acid and 0.1M NaCl according to specifications of standard ISO 10271:2011 [13]. To evaluate the corrosion behavior of specimens were performed the following procedure:

- electrochemical characterization of initial state of specimens (EIS) composed from the following tests: open circuit potential (OPC) monitoring for 10 min (up to quasi steady state).
- stationary immersion during 168 of hours.

Polarization curves were acquired starting from -1V/sce up to +1.5V/sce with a potential scanning rate of $1mVs^{-1}$. Tafel curves were made between ± 250mV/OPC with $1mVs^{-1}$ potential scanning rate. As electrochemical cells were used Teflon sterile beakers and the temperature was maintained at 37°C using Termostat incubator TC 25 Caloris.

Results and discussions

Phase analysis and microstructure

The composition of the obtained biomaterial alloy was established by EOS, as it is presented in table 1. All results are presented as the average of 3 measurements.

---

* *email: andrapredescu@yahoo.com; Phone: +40 21 402 98 29 / 21 316 95 64*

Table 1
CHEMICAL COMPOSITION OF BIOMATERIAL ALLOY

Elements	Ti	Nb	Fe
Composition, wt, %	62.48	25.92	11.60

The quantitative analysis confirms the efficiency of the levitation melting process under argon atmosphere that reveals a high compositional homogeneity, without impurities. Within this experiment, the induction melting and casting processes are strictly controlled by Ar atmosphere and cooled copper ingot stability. During this process, becomes impossible that the material to be contaminated with elements like C, H, O, N which could determine the fragility of the alloy. The obtained results from table 1 confirm this observation.

Figure 1 shows the XRD profiles of the titanium alloys for both applied cooling rates. The diffraction patterns reveal the presence of a bi-phasic structure, composed of α+ β Ti. The height of maximum intensity peak in diffraction pattern is not always a clear indicative referring to proportional quantity of identified phase. The complementary suggestions will be brought by SEM investigation. Moreover, the fact that the cooling rate has an influence on the fineness degree of the structure is demonstrated by calculus of crystallite size, using Debye-Scherrer's relation, presented below:

$$\tau = \frac{K\lambda}{\beta cos\theta} \qquad (1)$$

where: τ is the mean size of the ordered (crystalline) domains, K is a dimensionless shape factor, λ is the X-ray wavelength, β is the line broadening at half of the maximum intensity (FWHM), θ is the Bragg angle.

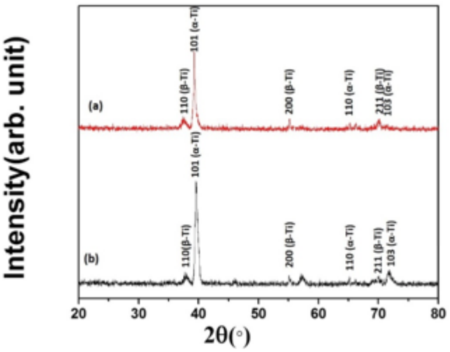

Fig. 1. XRD patterns for (a) *sample A1*(slow cooling) and (b) *sample A2* (fast cooling) of Ti-Nb-Fe alloy.

If we compare the crystallite sizes of each phase for both elaborated materials, it is easy to observe that if the alloy was slowly cooled (*sample A1*) the α and β phases have a higher crystallite size: =α - 46.81 nm and β-31.15 nm. In the case of the fast cooled alloy (*sample A2*) the structure is finer with crystallite size: α-27.51 nm and β - 16.12 nm. Therefore, increasing cooling rate from liquid state the structure becomes clearly finer.

The SEM investigation completes the X-ray diffraction results. It is obvious to observe that both cooling rates determine a biphasic structure (α+β), with α light and β dark grains. The SEM images confirm the finer structure for the fast cooling rates *(sample A2)*, completing the structure information that β phase is present in a higher proportion. In both situations the α-solid solution presents a dendritic distribution. It is important to note that the dendritic morphology depends on the cooling rate too: in the first case the dendrites have a coarser distribution *(sample A1)*, while in the second the morphology is much finer *(sample A2)*. The microstructure can be observed in figure 2.

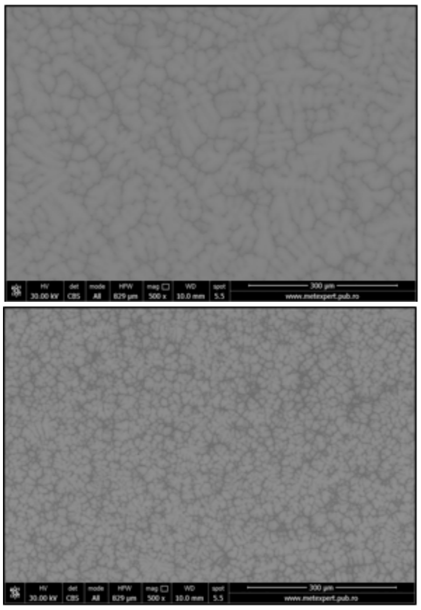

Fig. 2. SEM images for *sample A1*(slow cooling)-up and *sample A2* (fast cooling)-down of Ti-Nb-Fe alloy

J.M. Chaves et. al. [7] have analyzed similar microstructures in the Ti-Nb-Fe system, in which Nb content was gradually modified, the Fe composition being maintained at approximately 3 wt%. In his study, the SEM analysis revealed a surface not completely compact, the presence of a fair amount of defects being observed. But in our case, a higher content of Fe (e.g 11.6 wt% Fe) made possible the obtaining of a structure without any visible defects under SEM analysis deducting that the purposed induced a superior quality of the material. Another useful information which is present in the paper [14] refers to the high solubility of Fe in β-Ti polymorphic form. Consulting the equilibrium diagram Ti-Fe it is easy to observe the β-Ti phase stabilizer character of Fe and to attest its high solubility in β-Ti lattice. In conformity with these observations, titanium alloys with Nb and Fe have important mechanical properties and a better corrosion resistance, as it is emphasized in the papers [15]. Concretely, Fe content affects positively the critical passivation current density, inducing in material a higher corrosion resistance [11, 15, 16]. All this information will be retained for our corrosion investigation.

Corrosion tests

The main electrochemical parameters for corrosion behavior are corrosion potential and corrosion current density. Corrosion potential is a thermodynamic potential which offer information about the material tendency to passivate or on the contrary to corrode. When the corrosion potential moves to the electropositive values, the material tends to go into a passive state. Tafel analysis is to determine the corrosion current density at the intersection of the slopes in anodic and cathodic branches [17], respectively of the polarization curve plotted in semi - logarithmic coordinates around rest potential (±250mV) as is shown in the figure 3. From these data corrosion rates can be calculated.

As one can see in figure 3 the corrosion potential of fast cooled specimen is more electropositive (with about 300mV) than slow cooled Corrosion rate *V corr* express in μmy^{-1} was calculated using the relationship [18] :

$$V_{cor} = 0.00327A.icor / zp$$

where: A is average atomic weight; i_{cor} = corrosion density current in [Acm^{-2}]; z = valence; ρ=density in $g.cm^{-3}$.

The main corrosion parameters extracted from polarization curves are listed in the table 2 for both studied specimens.

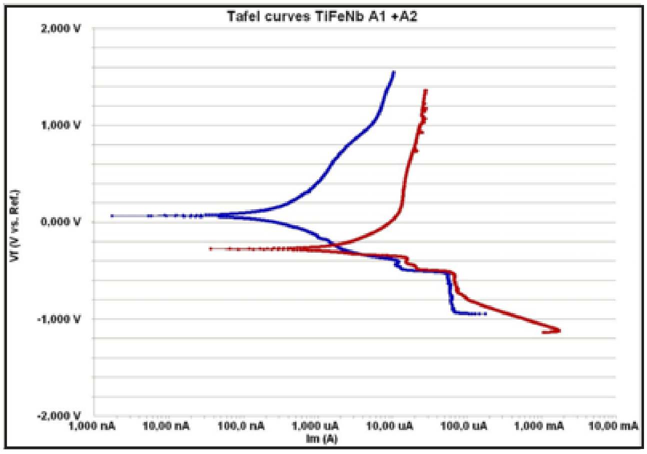

Fig. 3. The Tafel curves of cast TiNbFe specimens acquired in 0.1M lactic acid +0.1M NaCl at 37°C. A1-slow cooling; A2 fast cooling specimen

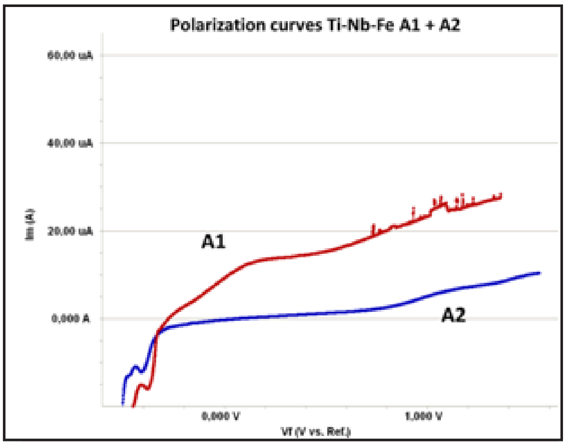

Fig. 4 The anodic polarization curves of cast TiNbFe alloy, 0.1M lactic acid +0.1M NaCl solution at 37°C acquired with $1 mVs^{-1}$ between 0.5V/sce and 1.5V/SCE

Table 2
THE MAIN CORROSION PARAMETERS FROM TAFEL CURVES PERFORMED IN 0.1M LACTIC ACID +0.1M NaCl at 37°C

Specimen	Ecorr [mv/sce]	icorr [µAcm-2]	Anodic slope V/decade	Catodic slope V/decade	Corrosion rate μmy^{-1}
A1 (slow cooled)	-276	2.270	0.432	0.140	8.30
A2 (fast cooled)	66	0.712	1.800	0.600	2.54

Analyzing the electrochemical parameters we appreciate the fact that the A2 is the more resistant specimen, the corrosion rate being almost three times exclusive. According to the BS EN ISO 8044: 2015 [19] the A2 specimen could be included in the group of corrosion resistance *very stable.* This behavior is in agreement with its microstructure.

The anodic polarization curves, presented in figure 4 show a typical shape for titanium alloys with the obvious trend to passivity. It is interesting to highlight the specimen A1 (slow cooled): at potentials more electropositive than + 1V it presents some small de-passivation and re-passivation picks, probably because of transpasivity to the iron, but no breakdown potential was observed. Anyway, the polarization curve aspect of the specimen A2 (fast cooled) justifies a favorable behavior to pitting corrosion.

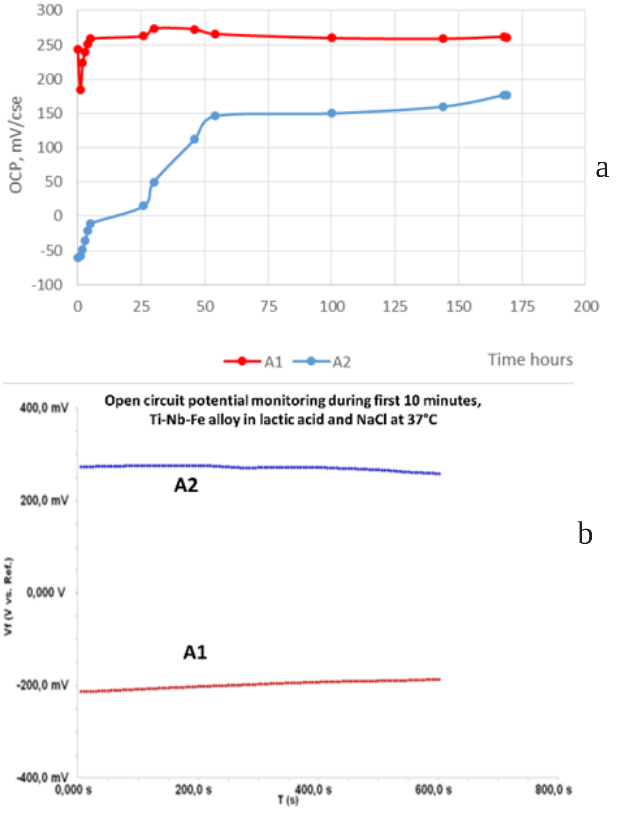

Fig.5. (a) OPC evolution during 168 h; (b) the OCP evolution during the first 10 min of immersion

Open circuit potential monitoring during 168 h in imersion of 0.1 M lactic acid and 0.1 M NaCl solution at 37°C is presented in figure 5 (a).

As can be seen from the figure 5 (b) the open circuit potential of the fast cooled specimen (A2) is more electropositive with about 300 mV compared with those of the slow cooled specimen (A1) even in the first minutes of immersion. Instead, during 168 h of immersion, the surface of specimen A2 revealed a very stable surface behavior, the potential reaches a steady state value around +250mV/sce, while the OPC of specimen A1 tends toward electropositive values. This information remains in correlation with other experimental data, pointing out the beneficial influence of controlled cooling cast technology in our case.

Conclusions

The paper proposes a new biomaterial from system Ti-Nb-Fe, in order to eliminate the toxic elements (such as Al or V) and to maintain the corrosion resistance to a high level. The new metallic biomaterial was realized in a cold crucible levitation melting furnace under argon atmosphere, able to achieve a high homogeneity and purity and to control the casting structure. The versatility of the furnace allows applying from liquid state of more cooling rates. The experiments include two representative values: 40°C/min for slow cooling and 160°C/min for fast cooling, both conditions generating particular structures. The XRD and SEM investigations demonstrated that the alloy has a biphasic $\alpha+\beta$ structure, despite the cooling rate. The α structure shows a tendency for dendritic crystallization and the global morphology is directly influenced by the cooling rate. A faster cooling rate leads to a more finely distributed structure, but having in the same time a higher proportion of β phase. All these aspects are sustained by the calculus of crystallite size and the SEM morphology. The β phase alloying with Nb and Fe is considered a favorable structure referring to the new Ti-based biomaterials due to its superior mechanical properties and optimal corrosion behavior. The tests of corrosion resistance were carried-out in standardized conditions (0.1M lactic acid +0.1M NaCl solution at 37°C). Electrochemical evaluation (Tafel curves, Polarization curves, corrosion rate *v corr*), Electrochemical impedance spectroscopy (Bode diagrams) and Open Circuit Potential evolution during 168 hours of immersion were the essential elements of the study. In all cases, without exception, the structure obtained by faster cooling rate (α+β-majoritary) had a superior corrosion behavior. Due to its properties, we consider that purposed alloy Ti - 62.48%, Nb- 25.92%, Fe-11.6% is a promising based-Titanium alloy with a increased biocompatibility. Besides, this alloy is framed in actual research recommending β (mono or predominantly β) structure because it has better biocompatibility. Important to point-out becomes the fact that the lower Nb content leads to a smaller production cost.

Acknowledgment: The work has been funded by the Increase of Economic Competitiveness Program through the Financial Agreement POSCCE ID Project: 1799 / 2015, SMIS 48589 and the PN III Proiect 87-BG/2016 : Enhanced technology for the elaboration of high purity materials aimed at infrastructure and transport special applications.

References

1. XU, L., CHEN, Y., LIU, Z.G., KONG, F., J. Alloys Compd., **453**, 2008, p. 320.
2. NIINOMI, M., NAKAI, M., HIEDA, J., Acta Biomater., **8**, 2012, p.3888.
3. STANCIULESCU M., ABRUDEANU M., GALATANU A., CARLAN P., MIHALACHE M., Rev. Chim.(Bucharest), **68**, no. 5, 2017, p. 1109.
4. HO, W.-F., PAN, C.-H., WU, S.-C., HSU, H.-C., J. Alloys Compd., **472**, 2009, p. 546.
5. KURODA, D., NIINOMI, M., MORINAGA, M., KATO, Y., YASHIRO, T., Mater. Sci. Eng. A**, 243**, 1998, p. 244.
6. GEPREEL, M.A.-H., NIINOMI, M., J. Mech. Behav. Biomed. Mater., **20**, 2013, p. 407.
7. CHAVES, J.M., FLORENCIO, O., SILVA JR, P.S., MARQUES, P.W.B., AFONSO, C.R.M., J. Mech. Behav. Biomed. Mater., **46**, 2015, p.184.
8. LI, Y., YANG, C., ZHAO, H., QU, S., LI, X., LI Y., Materials, **7**, 2014, p. 1709.
9. LEE, C.M., JU, C.P., CHERN LIN, J.H., J. Oral Rehabil., **29**, 2002, p. 314.
10. LOPES, \E.S.N., SALVADOR, C.A.F., ANDRADE, D.R., CREMASCO, A., CAMPO, K.N., CARAM, R., Metall. Mater. Trans. A, **47**, 2016, p. 3213.
11. MARTIN, E., MANCEUR, A., POLIZU, S., SAVADOGO, O., WU, M.H., YAHIA, L.H., Bio-Med. Mater. Eng., **16**, 2006, p.171.
12. ZHANG, D., MAO, Y., LI, Y., LI, J., YUAN, M., LIN, J., Mater. Sci. Eng.: A, **559**, 2013, p.706.
13.*** ISO 10271:2011 Dentistry - Corrosion test methods for metallic materials.
14. GONZALEZ, J.E.G., MIRZA-ROSCA, J.C., J. Electroanal. Chem., **471**, 1999, p. 109.
15. MOHAMMED, M.T., KHAN, Z.A., SIDDIQUEE, A.N., Int. J. Chem. Mol. Nucl. Mater. Metall. Eng, **8,** 2014, p. 788.
16. IONITA D., POPESCU B., DEMETRESCU I., Rev. Chim.(Bucharest), **60**, 2009, p. 1270.
17. VASILESCU E., DROB P., VASILESCU C., MARECI D., MIRZA-ROSCA J.C., Rev. Chim.(Bucharest), **61,** 2010, p. 660.
18. VASILESCU, E., DROB, P., RADUCANU, D., DAN, I., VASILESCU, C., Rev. Chim.(Bucharest), **60**, 2009, p. 241.
19. *** BS EN ISO 8044: 2015 - Corrosion of metals and alloys. Basic terms and definitions.

Manuscript received: 21.06.2017